Materials Science & Engineering C 98 (2019) 515–523

Contents lists available at ScienceDirect

Materials Science & Engineering C

journal homepage: www.elsevier.com/locate/msec

Single-walled carbon nanotube based coating modified with reduced graphene oxide for the design of amperometric biosensors

Jurgis Barkauskas[a], Lina Mikoliunaite[b], Ieva Paklonskaite[a], Povilas Genys[b], Jurate Jolanta Petroniene[b], Inga Morkvenaite-Vilkonciene[b,d], Almira Ramanaviciene[c], Urte Samukaite-Bubniene[b], Arunas Ramanavicius[b,e,*]

[a] Department of Inorganic Chemistry, Institute of Chemistry, Faculty of Chemistry and Geosciences, Vilnius University, Naugarduko 24, LT-03225 Vilnius, Lithuania
[b] Department of Physical Chemistry, Institute of Chemistry, Faculty of Chemistry and Geosciences, Vilnius University, Naugarduko 24, LT-03225 Vilnius, Lithuania
[c] NanoTechnas – Centre of Nanotechnology and Materials Science, Faculty of Chemistry and Geosciences, Vilnius University, Naugarduko 24, LT-03225 Vilnius, Lithuania
[d] Department of Electrochemical Material Science, State Research Institute Center for Physical Sciences and Technology, Sauletekio av. 3, LT-10222 Vilnius, Lithuania
[e] Laboratory of NanoBioTechnology, Institute of Semiconductor Physics, State Research Institute Center for Physical Sciences and Technology, Sauletekio av. 3, LT-10222 Vilnius, Lithuania

ARTICLE INFO

Keywords:
Single-walled carbon nanotubes
Graphene oxide
Polycarbonate membrane
Amperometric glucose biosensor
Glucose oxidase

ABSTRACT

In this study a polycarbonate filter membrane (PcFM) with 400 nm diameter holes was covered/protruded by single walled carbon nanotubes (SWCNT) and then formed PcFM/SWCNT structure was covered by thin layer of graphene oxide (GO) or reduced graphene oxide (rGO) in order to get the multilayered PcFM/SWCNT/GO and PcFM/SWCNT/rGO coatings, respectively. It was determined that the SWCNTs filaments were able to form a layer on the polycarbonate membrane having a number of carbon nanotube arranged in different orientations. A fraction of SWCNT filaments protruded through the holes of polycarbonate membrane and in such way significantly enhanced the adhesion of SWCNT-based layer and provided electrical conductivity across the PcFM. Atomic force microscopy (AFM), scanning electron microscopy (SEM) images and Raman spectroscopy-based evaluation revealed the characteristic morphology features: wide distribution of height profile, separate GO/rGO flakes on the top of PcFM/SWCNT/GO structure and close attachment of rGO flakes on the top of multilayered PcFM/SWCNT/rGO coating. Performed contact angle measurement (CAM) enabled to determine the surface energy components and wettability data of prepared coatings. Both PcFM/SWCNT/GO and PcFM/SWCNT/rGO coatings were modified with glucose oxidase (GOx). Amperometric measurements revealed that multilayered PcFM/SWCNT/rGO/GOx coating is the most suitable structure for glucose biosensor design.

1. Introduction

The transducing system is a critical part for a biosensor. In recent years achievements in the field of nanotechnology have made a significant impact on the design of advanced transducers for biosensors. Various nanomaterials such as gold nanoparticles [1], carbon nanomaterials [2–4] metallic nanoparticles [1,5,6], nanostructured conducting or redox-able polymers [7–9] have been applied to advance the performance of biosensors. Some of these nanomaterials substantially improve the quality, accuracy, reproducibility, detection limits, exploitation time, and reliability of biosensors. The dimensions of some nanoparticles are in the same range as that of enzymes, therefore, in some cases enzymes can be trapped in the cavities between these nanomaterials, which can serve as excellent matrixes for the enzyme immobilization. The combination of surface chemistry and enzymatic catalysis provides a great potential for reliable biosensors [10]. Among these materials carbon-based nanomaterials (CNMs) are widely used in biosensors as conducting component of transducer. Many CNMs have diverse and robust electronic properties as well as tunable opportunities of surface chemistry. In addition to these properties, an electrochemical activity of CNMs is exploited in biosensorics. The application of carbon-based quantum dots, carbon nanotubes (CNTs), graphene, graphene oxide (GO), has been reported [11]. Furthermore, the promise of cheap and disposable biosensors have been aided by developments in screen printed CNMs-based electrodes using carbon 'inks' [11]. However, a necessity to understand more precisely the interaction between the

* Corresponding author at: Department of Physical Chemistry, Institute of Chemistry, Faculty of Chemistry and Geosciences, Vilnius University, Naugarduko 24, LT-03225 Vilnius, Lithuania.
E-mail address: arunas.ramanavicius@chf.vu.lt (A. Ramanavicius).

https://doi.org/10.1016/j.msec.2019.01.005
Received 20 April 2018; Received in revised form 12 December 2018; Accepted 2 January 2019
Available online 03 January 2019
0928-4931/

protein and CNM surface still remains.

Single- and multi-walled CNTs (SWCNT, MWCNT) were utilized in transducer systems of various biosensors having aim to exploit their nanoscale dimensions, electro catalytic properties, and high surface area. Among the most significant advantages promoting the use of CNTs (especially, SWCNTs) in biosensors are their small diameter-to-length ratio, which allocates a close contact between the enzyme and an electro-conductive CNT [12]. CNTs can act as electron-relays, which can promote a direct electron transfer from enzymes' active sites. The biosensor nanoelectrode arrays made of CNTs are reported for various substrates [13]. These arrays produce higher currents in comparison with a single nanoelectrode. In the area of point-of-care biosensors, CNT forests have been utilized to lower H_2O_2 limits of detection down to the pico-molar range [14]. Novel nanotechnologies such as soft lithography, nanoimprint lithography, and highly ordered porous anodizing alumina template were used to achieve tunable and predictable well-ordered structures to prepare the CNT nanoelectrode arrays [13]. The immobilization of enzyme on CNTs is a key technology, which allows benefit from advantages of applied CNT. Non-covalent immobilization has been studied more intensively in comparison with the covalent methods due to its less destructive influence on enzyme's structure and simple immobilization procedure. During the covalent immobilization, specific functional groups are attached to the ends or side-walls of CNTs [15]. However, no universal enzyme supporting structure is available and therefore optimal immobilization method differs from enzyme to enzyme. Nonetheless, defined number of problems related to the preparation and application of CNT in biosensor design still remain. Among these there is the modification of CNTs in a better controlled way, e.g., separation of non-conducting, semi-conducting and well-conducting fractions of nanotubes, doping of CNTs with heteroatoms, synthesis of CNTs uniform in shape, length and number of formed walls, etc.

GO is a water-soluble derivative of graphene with double-sided geometry. It serves as an excellent substrate for the loading of biomolecules used in biosensors. GO is the precursor of reduced GO (rGO), which can be produced using different chemical, electrochemical or thermal synthesis protocols. Both GO and rGO can serve as an excellent immobilization platform for enzymes, antibodies or DNA. Through the interactions of GO and rGO with enzymes, proteins, or short-chain peptides, more complicated supramolecular architectures were assembled. Some of the as-obtained conjugates showed unique chemical properties that were found to be applicable in biosensorics [16]. Among the issues to be resolved using GO and rGO in biosensor design several problems should be mentioned. One of them is the detailed characterization of these materials, especially the distribution of oxygen-containing groups, which are crucial for both immobilization and interaction with enzyme molecules. The problem remains how to synthesize the individual graphene sheets of controllable size and quality. Control of conductivity, number of layers, and shape are also important factors for the application of these materials in biosensors.

The aims of this research were: (i) to prepare the hybrid (PcFM/SWCNT/GO and PcFM/SWCNT/rGO) structures, based on a hole-containing polycarbonate membrane (PcFM) covered/protruded by single walled carbon nanotubes and modified by a thin layer of graphene oxide (GO) or reduced graphene oxide (rGO), respectively; (ii) to explore synergistic effects of CNTs with GO or rGO; (iii) to evaluate the suitability of PcFM/SWCNT/GO and PcFM/SWCNT/rGO structures for glucose oxidase (GOx) immobilization and the applicability of such system in amperometric glucose biosensors.

2. Experimental

2.1. Materials

Glucose oxidase (EC 1.1.3.4, type VII, from *Aspergillus Niger*, 215.266 unit's mg^{-1} protein) and 25% glutaraldehyde solution were purchased from Fluka Chemie GmbH (Buchs, Switzerland). D-(+)-Glucose was obtained from Carl Roth GmbH (Karlsruhe, Germany). Before investigations, glucose solution was allowed to mutarotate overnight. All solutions were prepared using distilled water. Sodium acetate trihydrate, potassium chloride, sodium dihydrogen phosphate monohydrate, and disodium hydrogen phosphate dodecahydrate were obtained from Reanal (Budapest, Hungary) and Lachema (Neratovice, Czech Republic). Buffer solution (A-PBS) was prepared with 0.05 M CH_3COONa, 0.05 M NaH_2PO_4, 0.05 M Na_2HPO_4, and 0.1 M KCl. *N*-methylfenazin methosulphate (FMS) was obtained from Applichem, Germany. 40.0 mg/mL FMS solution was prepared in deionized water.

2.2. Preparation Of PcFM/SWCNT/GO structures

2.2.1. Preparation of CNT suspension

0.05 g of SWCNT powder (Cheap Nanotubes Inc.) and 0.1 g of Tween-80 (Merck KGaA, Germany) was placed in a beaker, poured with 25 mL of distilled water and left for 12 h. Later, the suspension was sonicated for 3 h using a desintegrator VCX 130 PB, SONYCS VibraCell, at 12% sonication amplitude. After the sonication, suspension was diluted by adding of distilled water up to 100 mL, placed in a glass beaker and sonicated again for 3 h at 15% amplitude. Concentration of the prepared SWCNT stock suspension was equal to $5.0\ 10^{-4}$ g/mL. It was used for the preparation of diluted SWCNT suspension ($5\ 10^{-5}$ g/mL) by dilution and subsequent sonication for 3 h. Prepared diluted SWCNT suspension was protruded through a loose cotton-wool plug in order to remove large SWCNT aggregates from diluted SWCNT suspension before use.

2.2.2. Synthesis of graphene oxide (GO)

GO was synthesized from the natural graphite by synthesis protocol reported earlier [17]. In a typical experiment, graphite powder was treated with concentrated H_2SO_4, $K_2S_2O_8$ and P_2O_5 [17]. Then, this pre-oxidized graphite was further oxidized by Hummers method [18].

2.2.3. Preparation of GO suspension

0.05 g of GO synthesized in the laboratory and 10 mL of distilled water was mixed in a small beaker and left for swelling at the room temperature for 24 h in a shaker. After that the mixture was sonicated for 1 h at 12% sonication amplitude. Prepared suspension was diluted up to 100 mL and sonicated again for 1 h at 15% amplitude. 1.00 mL of prepared suspension was diluted in a measuring flask up to 100 mL, poured into a beaker and sonicated for 1 h at 15% amplitude. Obtained diluted GO suspension ($5\ 10^{-6}$ g/mL) was used for the formation of SWCNT/GO coatings on the surface of PcFM surface.

2.2.4. Preparation of SWCNT, SWCNT/GO and SWCNT/rGO coatings

SWCNT coatings were prepared on the polycarbonate filter membrane (PcFM) (Merck Millipore Ltd., hole diameter 400 nm). The preparation procedure is described in more detail elsewhere [4]. The average thickness of prepared SWCNT coating was of 400 nm. Deposition of GO flakes on the surface of SWCNT coating was carried out from the aqueous GO solutions using the same protrusion procedure (SWCNT/GO coatings). An aliquot of diluted GO suspension GO (12 mL) was protruded through the SWCNT coating. The average thickness of formed GO layer on surface of SWCNT coating was equal to 20 nm. SWCNT/GO coatings were annealed at temperatures up to 160 °C in an oven SNOL 8,2/1100 developed in AB Utenos elektrotechnika, (Lithuania), in order to obtain a better conductivity due to the thermal reduction of GO as well as better adhesion of GO flakes to the SWCNT underlayer (SWCNT/rGO coatings). The rate of annealing was maintained equal to 20 °C/h.

2.2.5. Immobilization of glucose oxidase (GOx)

Enzyme GOx was immobilized onto PcFM/SWCNT, PcFM/SWCNT/GO and PcFM/SWCST/rGO structures by the same procedure. 10 μL of

20 mg/ mL solution of GOx in A-PBS, pH 7, was deposited on modified surface and it was dried at room temperature. Then GOx-modified surface of PcFM/SWCNT, PcFM/SWCNT/GO or PcFM/SWCST/rGO was treated by glutaraldehyde vapor by keeping it in a closed vessel over a 25% solution of glutaraldehyde for 10 min. During this step, the amino groups of the enzyme were interacting with aldehyde groups what leaded to covalent immobilization of the enzyme [15].

2.2.6. Preparation of the electrodes for amperometric biosensor

Graphite rod electrode (GR) (3.0 mm diameter; 30 mm length, 99.999%, Sigma-Aldrich, Germany) was polished using rough and smooth emery paper up to shining surface and then it was washed with copious amount of distilled water. Later electrode was covered with PcFM/SWCNT/rGO membrane and sides were confined with the tight plastic tube. Several different membrane immobilization techniques were chosen: membrane was placed: a) conducting side on top, b) crumbled with conducting side outside or c) conducting side inside. On the modified electrode 3 times of 3 μL, 10 mg/mL GOx enzyme solution prepared in acetate-phosphate buffer pH 6.0 was dropped. Each next drop was added only after the previous one dried. The modified electrode was stored for 15 min over a 25% solution of glutaraldehyde in a closed vessel. For the comparison an electrode without SWCNT coating (GR/GOx electrode) was prepared in the same manner, as it is described previously, only omitting the formation of SWCNT layer.

2.3. Characterization

2.3.1. Conductivity measurements

Conductivity measurements of PcFM/SWCNT structures were carried out using a multimeter (Mastech M-9803R) with two types of measurement cells: (i) a two-electrode based electrochemical cell and (ii) a four-electrode based electrochemical cell. The Ag contacts were used in both types of cells. Two-electrode cell was employed for the measurement of resistivity across (one electrode was connected to the SWCNT-modified and another one – to unmodified side of polycarbonate membrane) and along (both electrodes on the SWCNT-based side) the electro-conductive coating. A four-electrode cell was used only for the resistivity measurements along the SWCNT-based coating. For each type of cell, 10 specimens of SWCNT-based coatings were tested by repeating each measurement for 3 times.

2.3.2. Contact angle measurements. (CAM)

A CAM equipment CAM200 (Finland) with computer control and appropriate software was used for the experiment. The accepted contact angle measurement technique is based on the theory proposed by van Oss and co-workers [19]. This method is referred as an acid-base method elsewhere [20]. For this purpose, three solvents of different polarity (water, glycerol and 1-bromnaphtalene) were used. For the calculation of total surface energy such equation was applied:

$$\gamma_S^T = \gamma_S^{LW} + \gamma_S^{AB} \quad (1)$$

where $\gamma_S{}^{LW}$ is denoted as Lifschitz–van der Waals contribution ranked as the dispersive interactions, and $\gamma_S{}^{AB}$ occurs by means of acid-base interaction (e.g., hydrogen bond formation). In turn, $\gamma_S{}^{AB}$ it can be resolved into two components: acidic $\gamma_S{}^{+}$ and basic $\gamma_S{}^{-}$ ones, and the total surface energy can be written as:

$$\gamma_S^T = \gamma_S^{LW} + 2\sqrt{\gamma_S^+ \gamma_S^-} \quad (2)$$

Both the total surface energy and its components of SWCNT coatings were determined from the CAM data. The procedure of determination is described in more detail elsewhere [21].

The morphology of SWCNT and SWCNT/GO coatings was analyzed using atomic force microscopy (AFM) and scanning electron microscopy (SEM). Surface topography of polycarbonate membrane, PcFM/SWCNT and PcFM/SWCNT/GO was evaluated using atomic force microscope Bioscope Catalyst form Bruker, (Santa Barbara, USA). The Scan Asyst based on Peak Force Tapping mode equipped with the conventional silicon Scan Asyst Air AFM tip (resonance frequency 70 kHz, spring constant 0.4 N m^{-1}) was used. The images were obtained using NanoScope Analysis program provided by Bruker. SEM images were obtained using a Hitachi SU-70 microscope (Tokyo, Japan) at an accelerating voltage of 5.0 kV and magnifications of 25,000× and 50,000×.

The 2D Raman spectra of the SWCNT and SWCNT/GO coatings were obtained using a WITec Alpha300R Raman spectrometer with 532 nm excitation laser source.

2.3.3. Amperometric measurements

For electrochemical measurements, the potentiostat/galvanostat PGSTAT 30 (Autolab, Netherlands) equipped with reference $Ag/AgCl_{3M\ KCl}$ and counter platinum electrodes was applied. Firstly, the 20 mL cell was filled with 4750 μL of A-PBS and 250 μL of FMS. All the measurements were performed at $+0.3\ V$ working potential *v.s.* $Ag/AgCl_{3M\ KCl}$. During the measurement, certain amount of glucose solution was added to the cell continuously. The obtained amperometric signals were interpreted using Michaelis-Menten kinetics.

3. Results and discussion

Results of the resistivity measurement along the SWCNT coating using two-electrode and four-electrode cells are presented in Fig. 1a.

A statistical evaluation was used to compare both series of measurement, and statistical hypothesis was formulated: H_0 (null hypothesis) – two series of measurement are comparable, and H_1 (alternative hypothesis) – two series of measurement are non-comparable. Fisher distribution test was used for the evaluation and assessment results are presented in Table 1.

Result of the statistical evaluation is $F_{exp} > F\ (p; f1; f2)$, therefore the null-hypothesis was rejected. The alternative hypothesis is that the results of two measurement series are non-comparable. Considering the variance obtained using a two-electrode cell a conclusion can be drawn that results in this measurement are much less confident in comparison with that registered using a four-electrode cell. In a number of researches it was pointed out that the SWCNT in contact with a metal behave as Shottky barrier devices, even if CWCNTs are contacting with inert metals (Au, Pt, Pd) [22]. Results obtained in our research are in agreement with this observation. In one publication it was reported that the best quality of electrical contact between SWCNTs and electrode is achieved if SWCNTs are deposited on graphite or graphene based substrates [23]. This finding prompted the use of additional GO or reduced GO coating on the top of SWCNT in our studies with the aim for the further application in biosensors. Further electrical resistivity measurements along the SWCNT-based coating were carried out using a four-electrode cell.

SWCNT-based coatings formed on the porous polycarbonate membrane (PcFM/SWCNT) were annealed at different temperatures up to 180 °C. Changes in the structure were examined by measuring the resistivity along and across PcFM/SWCNT structure (Fig. 1b). Results obtained measuring the resistivity along the PcFM/SWCNT structure does not showed any significant dependence on the temperature. On the contrary, measurement across the PcFM/SWCNT structure revealed an obvious decrease in resistivity at higher temperatures. Therefore, we can predict that formed SWCNT coatings are of high structural anisotropy. Parallelly to the polycarbonate substrate, the SWCNT coatings are mainly isotropic, while in a perpendicular direction they show anisotropic properties. Supposedly, small fraction of SWCNTs during the preparation procedure fills the holes in the polycarbonate membrane, and some of SWCNTs even protrudes the holes. For this reason, the resistivity of SWCNTs across the coating is very high. During the annealing procedure, while the polycarbonate substrate is prone to shrinkage, the resistivity drops from 140 kΩ down to 7 kΩ. Based on

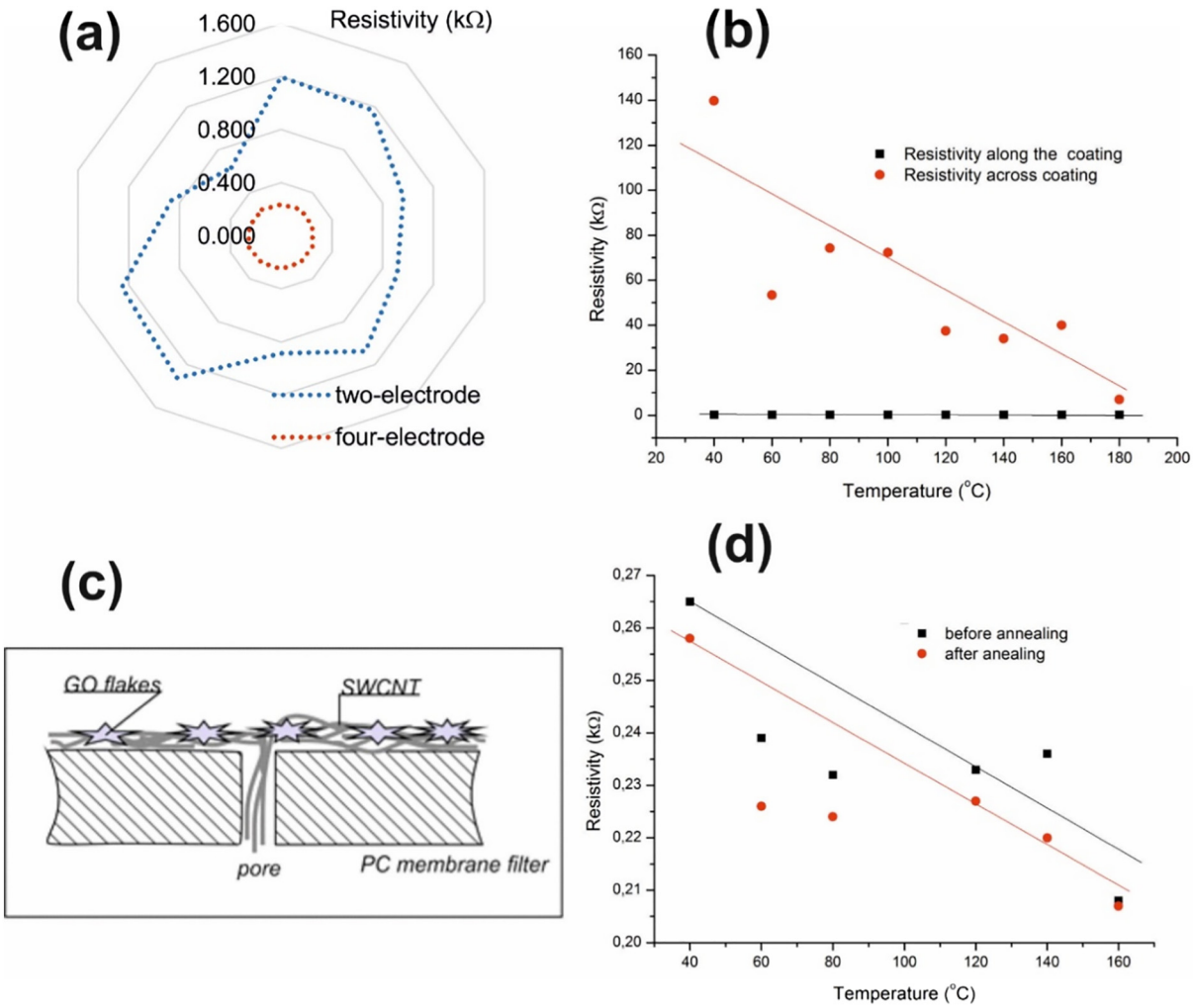

Fig. 1. Results of electrical resistivity measurements and distribution of SWCNT filaments and GO flakes on the surface of polycarbonate membrane. Electrical resistivity of SWCNT-based coatings by measuring along the coating with two-electrode and four-electrode based cells (a). Comparison of resistivity of annealed SWCNT-based coatings measuring along and across the coating (b). Distribution of SWCNT and GO flakes on the surface of polycarbonate membrane (c). Resistivity's of SWCNT/GO coatings along the surface before and after annealing (d).

Table 1
Statistical values of the Fisher analysis.

	Two-electrode cell	Four-electrode cell
Degrees of freedom– f_1; f_2	3; 9	3; 9
Variance - s^2	0.0453	0.0000357
Significance level - p	0.05	
$F_{exp} = s_1^2/s_2^2$	1268.536	
Standard value -$F(p;f_1;f_2)$	3.862	

these results, a structural model of the SWCNT coating on the polycarbonate substrate was proposed and it is represented in Fig. 1c.

Prepared PcFM/SWCNT/GO structures were annealed at the same temperatures as these without the GO coating. The resistivity data before and after annealing measured using a four-electrode cell are presented in Fig. 1d. Changes in the resistivity after annealing are insignificant, there is only a very weak correlation with the annealing temperature. Direct conductivity measurement leads to the conclusion that the modification of PcFM/SWCNT structure with GO as well as annealing procedure does not impair the electrical conductivity characteristics of the PcFM/SWCNT/GO based structure.

CAM data obtained for SWCNT coatings are presented in Fig. 2a and b.

The best wetting of pure nanotube surface is achieved with 1-bromonaphtalene (Fig. 2a and c). Wetting of both SWCNTs-based coatings with water depends on the temperature (Fig. 2a and c). The decrease of hydrophobicity is based on the influence of dispersing agent – Tween-80, which was used for the preparation of SWCNTs suspension used for the formation of coatings. Glycerol was determined as a poor-wetting liquid. At higher temperatures the wetting angle increases for all here tested liquids, what demonstrate the decrease of surface free energy of SWCNTs coating.

Surface free energy and its components (Fig. 2b) likewise undergo a characteristic change during the annealing procedure. Non-polar component γ_S^{LW} remains constant, while other components are reaching their maximum values at 140 °C. Basic interaction γ_S^- is much more significant in comparison to the acidic interaction γ_S^+ up to 180 °C. In conclusion, SWCNT coating should be considered as a polar surface with prevailing basic properties. At higher temperatures (180 °C) the γ_S^{AB} component decreases, and non-polar γ_S^{LW} component remains predominant.

CAM data for SWCNT/GO coatings are provided in Fig. 2c and d. Wetting of SWCNT/GO coatings with the same liquids differs from that of pristine SWCNTs coatings (Fig. 2c and a). For SWCNT/GO-based coatings all here determined wetting angles are scattered in a narrower range in comparison to pristine SWCNT-based coating where wetting angles are scattered from 15° (for 1-bromonaphtalene) to 75° (for glycerol). The values of wetting angle for the wetting of SWCNT/GO-based

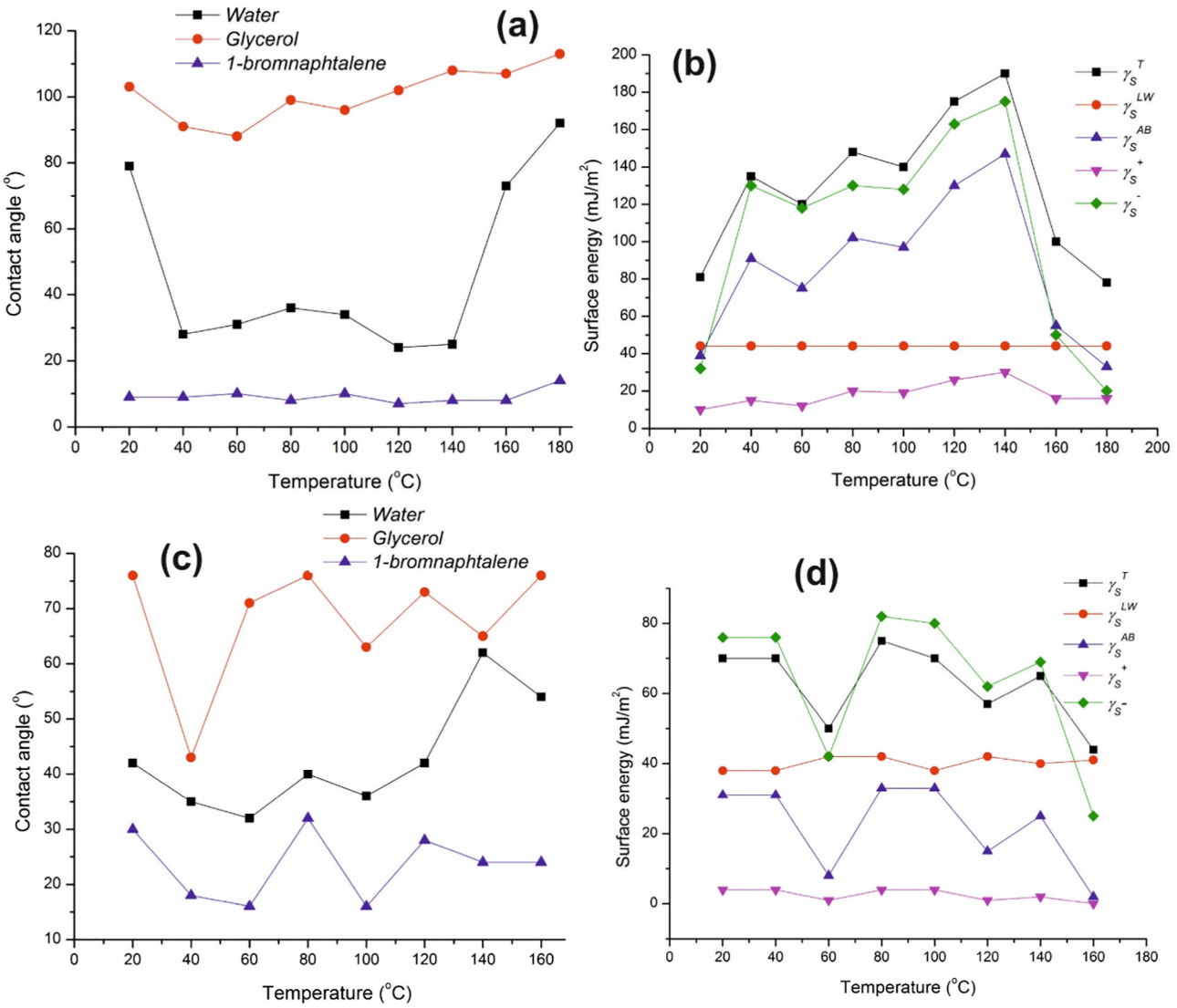

Fig. 2. CAM data and surface energy components of different SWCNT-based coatings: CAM data obtained for SWCNT coatings after the annealing of PcFM/SWCNT at different temperatures (a); Surface free energy (and its components) of SWCNT coatings after the annealing of PcFM/SWCNT at different temperatures (b); CAM data obtained for SWCNT/GO coatings after the annealing of PcFM/SWCNT/GO at different temperatures (c); Surface free energy (and its components) of SWCNT/GO coatings after the annealing of PcFM/SWCNT/GO at different temperatures (d).

coatings by water do not reach such high values as in the case of pristine SWCNT coatings. This should be determined by the influence of GO coating, which is formed over the SWCNT layer (Fig. 1c). Irregular changes in wetting angle at different temperatures can also be assigned to the reduction of GO. Similarly, the decrease of surface free energy and its polar components at 60 °C may occur due to the characteristic reduction of GO sheets and reconstruction of graphene structure. At higher temperatures (160 °C), as well as in the case of pristine SWCNT-based coatings (Fig. 2a), a predomination of non-polar γ^{SLW} component is observed.

It is well known that hydrophilic properties of carbon surface are closely related to the presence of oxygen-containing functional groups in a wide range of functional groups epoxy-groups are prevailing [24]. Considering CAM results along with the surface energy data it is possible to draw a conclusion that the annealing at 180 °C reduces the content both acidic and basic oxygen-containing functional groups, while basic epoxy groups are more resistant to the annealing procedure.

The AFM and SEM images of SWCNT and SWCNT/GO coatings are presented in Fig. 3.

Irregular distribution of SWCNTs on the polycarbonate membrane is observed (Fig. 3). The height scale of SWCNT coating shows a wide distribution through 330 nm (Fig. 3a). After additional modification of SWCNT coating by GO this distribution has slightly decreased down to 240 nm, because GO sheets tend to smooth a rough surface of SWCNT coating. Neither single nanotubes nor their conglomerations are observed in the AFM image of SWCNT/GO coating (Fig. 3b).

The SEM image of SWCNT protruded through the hole to the opposite side of polycarbonate membrane (Fig. 3c) confirms the hypothesis about the protrusion of SWCNT filaments across the holes of the polycarbonate based membrane. SEM images of SWCNT, SWCNT/GO and SWCNT/rGO coatings are shown in Fig. 3d, e and f. SEM images reveal the same regular patterns as these visualized by AFM. In SEM images it is possible to distinguish the tangled SWCNT agglomerations in the coating morphology. Single GO sheets are observed in SWCNT/GO coatings before the annealing, while after the annealing at +160 °C reduced GO sheets become more closely attached to the surface of SWCNT layer.

Raman spectroscopy and Raman imaging data of pristine and annealed coatings are presented in Fig. 4. In Fig. 4a four characteristic peaks of SWCNTs are observed at: ~1347 cm^{-1} (D-band), ~1590 cm^{-1} (G-band), ~2676 cm^{-1} (G′-band), ~264 cm^{-1} (RBM-band). From these results low I_D/I_G ratio has been determined, which confirms the non-

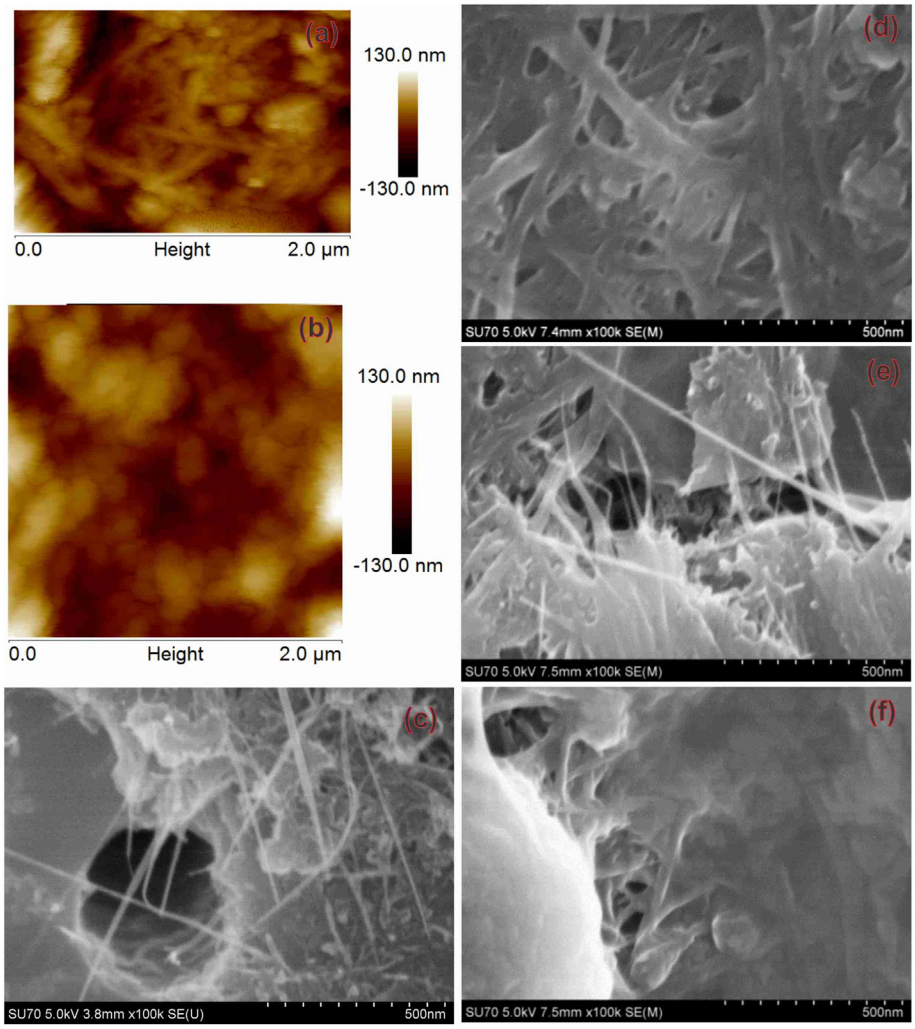

Fig. 3. The morphology of SWCNT-based coatings. AFM image of pristine SWCNT coating (a), AFM image of SWCNT/GO coating (b); SEM image of SWCNT coating from the opposite side of PcFM/SWCNT structure (c); SEM image of SWCNT from the front side of PcFM/SWCNT structure(d); SEM image of SWCNT/GO from the opposite side of PcFM/SWCNT/GO structure (e); SEM image of SWCNT/rGO from the opposite side of PcFM/SWCNT/rGO structure (f).

defective structure of SWCNTs used in the experiment. This ratio increases even more after the annealing, supposedly due to the annealing-based removal of Tween-80 molecules, which were used for stabilization of SWCNT suspension. The same characteristic peaks are observed for SWCNT/GO coating (Fig. 4b), though after the annealing at 160 °C the intensity of RBM-band is significantly reduced (Fig. 4a). This effect can be related to the establishment of advanced contact of reduced GO sheets with the surface of SWCNTs, which leads to the damping of RBM vibrations. Formation of close contact between SWCNT and GO after the annealing is also confirmed by SEM images.

In Fig. 4c, d, e and f Raman imaging patterns of prepared coatings (SWCNT, SWCNT annealed at 180 °C, SWCNT/GO and SWCNT/rGO) at four characteristic modes (RBM, D, G and G′) are presented, respectively. The brighter regions indicate the more intensive Raman scattering. Certain regularities are observed for different wavenumbers in various samples. Difference in the imaging results for pristine SWCNT coatings is observed dependent on the characteristic wavenumber (Fig. 4c). RBM and G′ responses are intensive and evenly distributed in a whole area, while D- and G-scattering is much less evenly distributed. This result confirms the hypothesis about uneven distribution of SWCNT in the coating, which is observed in the AFM images. After the annealing D- and G-scattering becomes more evenly distributed (Fig. 4d). Supposedly annealing is beneficial for the production of separated SWCNTs and observation of their response at D- and G-modes. AFM and SEM images (Figs. 3 and 4e) illustrate that the pristine SWCNT/GO coatings are smoother in comparison to pristine SWCNT based coating. Annealed SWCNT/rGO coating (Fig. 4f) become even smoother in comparison to the pristine SWCNT based one.

The applicability of SWCNT-modified membrane for the design of biosensor was evaluated (Fig. 5). Because the polycarbonate membrane has two differently modified sides, several different modification techniques were applied. The polycarbonate membrane side modified by SWCNT/rGO possessed better conductivity in comparison with side opposite side, because on the opposite side only a few SWCNTs crawled out from the holes of the membrane. The modified polycarbonate membranes were wrapped on a polished graphite rod electrode in two different ways: on the first type of electrodes, the membrane was placed in such way that the conducting side of membrane was in direct contact with graphite (GR) electrode (GR/SWCNT/rGO/GOx). On the second type of electrodes, the membrane was turned halfway leaving the nonconducting part inside and then placed on the electrode (GR/2SWCNT/rGO/GOx). The modification with enzyme glucose oxidase was performed in the same way. For the control measurements, the electrode without the membrane (GR/GOx) and the electrode with the membrane turned in half and conducting part inside were prepared (GR/NON-SWCNT/GOx).

The obtained results were interpreted using Michaelis-Menten kinetics and the fitted values are presented in Table 2. The results showed

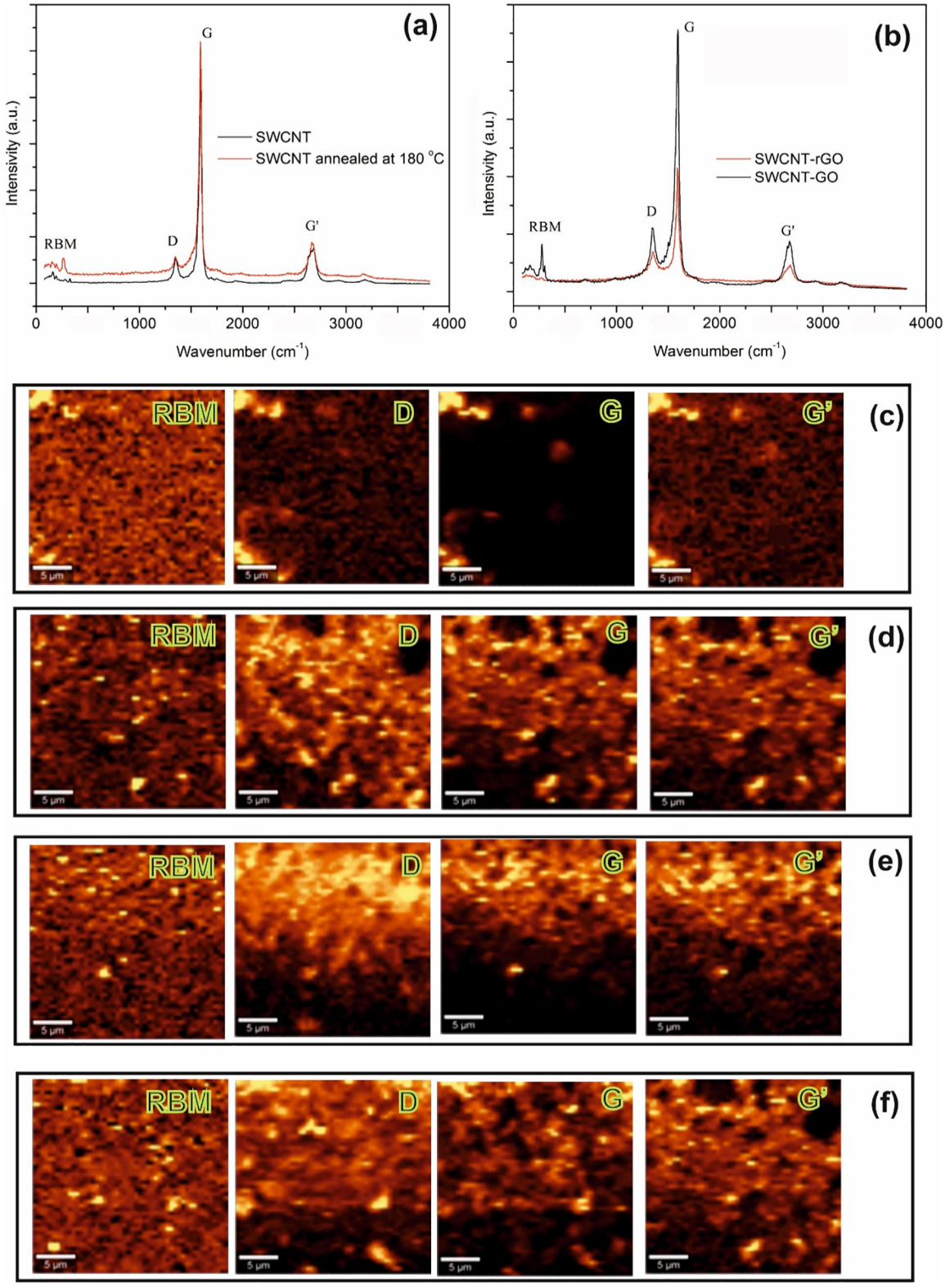

Fig. 4. Raman spectra and Raman imaging patterns of different SWCNT-based coatings. Raman spectra of: pristine and at 180 °C annealed SWCNT coatings – (a); SWCNT/GO and SWCNT/rGO (b). Raman imaging patterns at four different modes (RBM, D, G and G′): pristine SWCNT coating (c); SWCNT coating annealed at 180 °C (d); SWCNT/GO coating (e); SWCNT/rGO coating (f).

that GR/NON-SWCN/rGO/GOx electrode showed no significant signal, however for the other three types of electrodes (GR/2SWCNT/rGO/GOx, GR/SWCNT/rGO/GOx, GR/GOx), the obtained amperometric values were very similar. The GR/SWCNT/rGO/GOx electrode had slightly higher maximal current value (up to 8%) in comparison to GR/2SWCNT/rGO/GOx and GR/GOx electrodes and GR/2SWCNT/rGO/GOx showed the lowest K_M value, which is related to faster enzymatic reaction and lower influence of diffusion-based limitations on enzymatic kinetics determined for GR/2SWCNT/rGO/GOx electrode. Thus, the polycarbonate membrane with SWCNTs did not reduce the electron

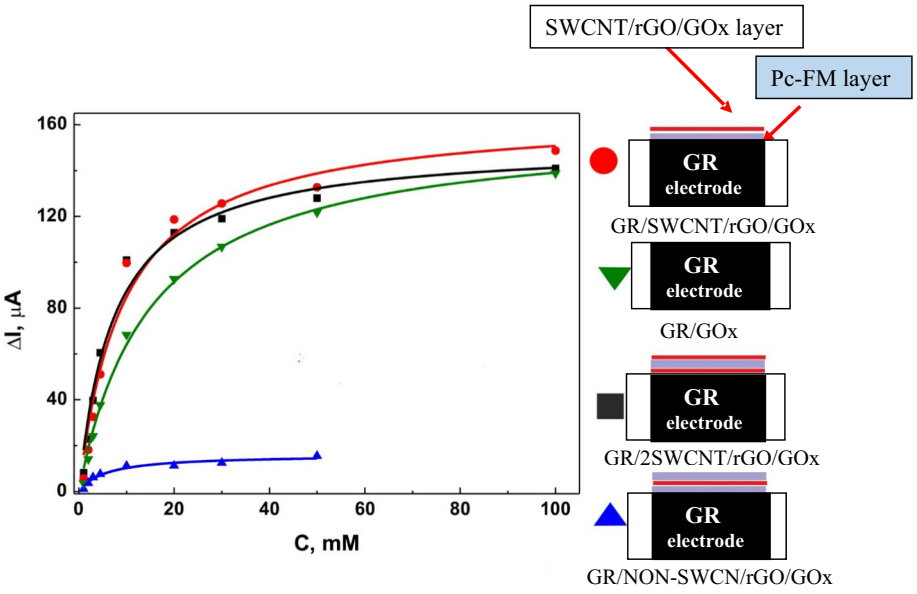

Fig. 5. Amperometric measurements of the carbon electrode modified with pristine SWCNT-covered polycarbonate membrane. Different modification techniques were used: membrane placed modified side on top (GR/SWCNT/rGO/GOx) (round dots); membrane turned halfway with conducting side outside (GR/2SWCNT/rGO/GOx) (squares) or inside (GR/NON-SWCN/rGO/GOx) (triangles) and compared with the graphite rod electrode without membrane (GR/GOx) (triangles).

Table 2
The Michaelis-Menten kinetic parameters of the electrodes prepared using different SWCNT-based polycarbonate membrane.

Electrode	K_M, mmol/L	I_{max}, μA	R^2
GR/2SWCNT/rGO/GOx	7.5	152.1	0.9838
GR/SWCNT/rGO/GOx	9.6	165.4	0.9819
GR/NON-SWCN/rGO/GOx	5.8	16.1	0.9706
GR/GOx	15.1	160.2	0.9960

Table 3
The Michaelis-Menten kinetic parameters of the electrodes, modified by GOx and CNT.

Electrode	K_M, mmol/L	Ref.
Nafion/GOx/Ag-Pdop@CNT/GCE	5.46	[25]
Au/POAP/CNT/GOx	18.8	[26]
GOx at PMMA–MWCNT(PDDA)/GOx–NFE	10.12	[27]
GOx immobilized Prussian blue/MWCNT nanocomposites	18	[27]
GOx immobilized on colloidal gold-MWCNT/Teflon	14.9	[27]
MWCNT/Teflon composite electrodes	30	
GR/2SWCNT/rGO/GOx	7.5	This work

Polydopamine (Pdop); glassy carbon electrode (GCE); POAP- Poly(o-Aminophenol); poly(diallyldimethylammonium chloride) (PDDA); nanofibrous electrode (NFE); multiwalled carbon nanotubes (MWCNT).

transfer rate from the enzyme to the electrode. The obtained parameters are almost the same as for GR/GOx electrode. These results indicate that the membrane can be efficiently used as a flexible electrode for enzymatic-amperometric biosensor design (Table 3).

3.1. Conclusions and future trends

SWCNT-based coatings (of ~400 nm thickness) were formed on the polycarbonate membranes punctured by 400 nm diameter holes using a protocol of filtration into solution. Formed SWCNT-modified polycarbonate membranes were applied as electrode coatings suitable for amperometric biosensors. SWCNT-modified polycarbonate membranes were modified additionally was covered by GO flakes (SWCNT/GO coatings) and some of such structures were subsequently annealed (SWCNT/rGO coatings). Produced coatings were investigated in order to identify their structure, some electrical and bio-electrochemical properties and surface chemistry. It was determined that SWCNT coatings have a high structural anisotropy while measuring the electrical conductivity along and across the coating. CAM measurements were used to investigate surface properties of prepared coatings. The SWCNT coating has been considered as a polar surface with prevailing basic properties. It was calculated that for annealed SWCNT coatings non-polar surface energy component becomes predominant. SWCNT/GO coatings are more basic and more hydrophilic due to the presence of GO sheets on the top of SWCNTs coating. For SWCNT/rGO-based coating, as well as for SWCNT-based coating, a predomination of non-polar component is observed. AFM and SEM images revealed the characteristic morphology features: wide distribution of height profile, presence of separated GO flakes on the surface of SWCNT layer in PcFM/SWCNT/GO structure and good attachment of rGO flakes on the surface of SWCNT in SWCNT/rGO. Raman spectra confirmed the interaction between SWCNTs and rGO flakes in PcFM/SWCNT/rGO structure and more even distribution of rGO flakes on surface of SWCNT in SWCNT/rGO coatings, which were formed by annealing at 160 °C. There are some positive indications that PcFM/SWCNT/rGO structures are prospective for the design of glucose biosensors.

Acknowledgements

This research is/was funded by the European Regional Development Fund according to the supported activity 'Research Projects Implemented by World-class Researcher Groups' under Measure No. 01.2.2-LMT-K-718.

References

[1] N. German, A. Ramanavicius, J. Voronovic, A. Ramanaviciene, Glucose biosensor based on glucose oxidase and gold nanoparticles of different sizes covered by polypyrrole layer, Colloid Surf. A 413 (2012) 224–230.
[2] M. Aramesh, P.A. Tran, K. Ostrikov, S. Prawer, Conformal nanocarbon coating of alumina nanocrystals for biosensing and bioimaging, Carbon 122 (2017) 422–427.
[3] B. Li, A. Yu, G. Lai, Self-assembly of phenoxyl-dextran on electrochemically reduced graphene oxide for nonenzymatic biosensing of glucose, Carbon 127 (2018) 202–208.
[4] J. Barkauskas, pH-dependent water penetration through CNT sub-layers arranged on the polycarbonate membrane filters, Carbon 48 (2010) 1858–1865.
[5] V. Mazeiko, A. Kausaite-Minkstimiene, A. Ramanaviciene, Z. Balevicius, A. Ramanavicius, Gold nanoparticle and conducting polymer – polyaniline – based nanocomposites for glucose biosensor design, Sensors Actuators B 189 (2013) 187–193.
[6] J. Yang, W. Tan, C. Chen, Y. Tao, Y. Qin, Y. Kong, Nonenzymatic glucose sensing by

CuO nanoparticles decorated nitrogen-doped graphene aerogel, Mater. Sci. Eng. C 78 (2017) 210–217.
[7] A. Ramanavicius, A. Kausaite, A. Ramanaviciene, Self-encapsulation of oxidases as a basic approach to tune upper detection limit of amperometric biosensors, Analyst 133 (2008) 1083–1089.
[8] Y. Oztekin, V. Krikstolaityte, A. Ramanaviciene, Z. Yazicigil, A. Ramanavicius, 1,10-Phenanthroline derivatives as mediators for glucose oxidase, Biosens. Bioelectron. 26 (2010) 267–270.
[9] S. Li, J.-X. Xiong, C.-X. Chen, F.-Q. Chu, Y. Kong, L.-H. Deng, Amperometric biosensor based on electrochemically reduced graphene oxide/poly(*m*-dihydroxybenzene) composites for glucose determination, Mater. Technol. 32 (2017) 1–6.
[10] Y. Liu, J. Yu, Oriented immobilization of proteins on solid supports for use in biosensors and biochips: a review, Microchim. Acta 183 (2016) 1–19.
[11] F.R. Baptista, S.A. Belhout, S. Giordani, S.J. Quinn, Recent developments in carbon nanomaterial sensors, Chem. Soc. Rev. 44 (2015) 4433–4453.
[12] J.J. Gooding, Nanostructuring electrodes with carbon nanotubes: a review on electrochemistry and applications for sensing, Electrochim. Acta 50 (2005) 3049–3060.
[13] Z. Zhu, L. Garcia-Gancedo, A.J. Flewitt, H. Xie, F. Moussy, W.I. Milne, A critical review of glucose biosensors based on carbon nanomaterials: carbon nanotubes and graphene, Sensors 12 (2012) 5996–6022.
[14] X. Yu, B. Munge, V. Patel, G. Jensen, A. Bhirde, J.D. Gong, S.N. Kim, et al., Carbon nanotube amplification strategies for highly sensitive immunodetection of cancer biomarkers, J. Am. Chem. Soc. 128 (2006) 11199–11205.
[15] W. Feng, P. Ji, Enzymes immobilized on carbon nanotubes, Biotechnol. Adv. 29 (2011) 889–895.
[16] S. Ding, A.A. Cargill, I.L. Medintz, J.C. Claussen, Increasing the activity of immobilized enzymes with nanoparticle conjugation, Curr. Opin. Biotechnol. 34 (2015) 242–250.
[17] X. Yan, J. Chen, J. Yang, Q. Xue, P. Miele, Fabrication of free-standing, electrochemically active, and biocompatible graphene oxide − polyaniline and graphene − polyaniline hybrid papers, Appl. Mater. Interfaces 9 (2010) 2521–2529.
[18] W.S. Hummers, R.E. Offeman, Preparation of graphitic oxide, J. Am. Chem. Soc. 80 (1958) 1339.
[19] C.J. van Oss, Interfacial Forces in Aqueous Media, second ed., Marcel Dekker, New York, 1994.
[20] A. Hollander, On the selection of test liquids for the evaluation of acid-base properties of solid-surfaces by contact-angle goniometry, J. Colloid Interface Sci. 169 (1995) 493–496.
[21] J. Barkauskas, I. Žaržojūtė, A. Kareiva, Production and contact angle measurement of nano-structured carbon coatings, Chem. Aust. 18 (2007) 12–16.
[22] Z. Chen, J. Appenzeller, J. Knoch, Y.M. Lin, P. Avouris, The role of metal − nanotube contact in the performance of carbon nanotube field-effect transistors, Nano Lett. 5 (2005) 1497–1502.
[23] W. Wang, S. Guo, M. Penchev, I. Ruiz, K.N. Bozhilov, D. Yan, M. Ozkan, C.S. Ozkan, Three dimensional few layer graphene and carbon nanotube foam architectures for high fidelity supercapacitors, Nano Energy 2 (2013) 294–303.
[24] L. Luo, T. Peng, M. Yuan, H. Sun, S. Dai, L. Wang, Preparation of graphite oxide containing different oxygen-containing functional groups and the study of ammonia gas sensitivity, Sensors 18 (2018) 3745–3760.
[25] Y. Wang, L. Liu, M. Li, S. Xu, F. Gao, Multifunctional carbon nanotubes for direct electrochemistry of glucose oxidase and glucose bioassay, Biosens. Bioelectron. 30 (2011) 107–111.
[26] D. Pan, J. Chen, S. Yao, W. Tao, L. Nie, An amperometric glucose biosensor based on glucose oxidase immobilized in electropolymerized poly(o-aminophenol) and carbon nanotubes composite film on a gold electrode, Anal. Sci. 21 (2005) 367–371.
[27] K.-M. Manesh, H.-T. Kim, P. Santhosh, A.-I. Gopalan, K.-P. Lee, A novel glucose biosensor based on immobilization of glucose oxidase into multiwall carbon nanotubes–polyelectrolyte-loaded electrospun nanofibrous membrane, Biosens. Bioelectron. 23 (2008) 771–779.